

At the limits of criticality-based quantum metrology: apparent super-Heisenberg scaling revisited

Marek M. Rams,¹ Piotr Sierant,¹ Omyoti Dutta,^{1,2} Paweł Horodecki,^{3,4} and Jakub Zakrzewski^{1,5}

¹*Instytut Fizyki im. Mariana Smoluchowskiego, Uniwersytet Jagielloński, Łojasiewicza 11, 30-348 Kraków, Poland **

²*Donostia International Physics Center DIPC, Paseo Manuel de Lardizabal 4, 20018 Donostia-San Sebastián, Spain.*

³*Faculty of Applied Physics and Mathematics, Gdańsk University of Technology,
ulica Gabriela Narutowicza 11/12, 80-233 Gdańsk, Poland*

⁴*National Quantum Information Center of Gdańsk,
ulica Władysława Andersa 27, 81-824 Sopot, Poland†*

⁵*Mark Kac Complex Systems Research Center, Uniwersytet Jagielloński, Kraków, Poland. ‡*

(Dated: February 14, 2022)

We address the question whether the super-Heisenberg scaling for quantum estimation is indeed realizable. We unify the results of two approaches. In the first one, the original system is compared with its copy rotated by the parameter dependent dynamics. If the parameter is coupled to the one-body part of the Hamiltonian the precision of its estimation is known to scale at most as N^{-1} (Heisenberg scaling) in terms of the number of elementary subsystems used, N . The second approach compares the overlap between the ground states of the parameter dependent Hamiltonian in critical systems, often leading to an apparent super-Heisenberg scaling. However, we point out that if one takes into account the scaling of time needed to perform the necessary operations, i.e. ensuring adiabaticity of the evolution, the Heisenberg limit given by the rotation scenario is recovered. We illustrate the general theory on a ferromagnetic Heisenberg spin chain example and show that it exhibits such super-Heisenberg scaling of ground state fidelity around the critical value of the parameter (magnetic field) governing the one-body part of the Hamiltonian. Even an elementary estimator represented by a single-site magnetization already outperforms the Heisenberg behavior providing the $N^{-1.5}$ scaling. In this case Fisher information sets the ultimate scaling as $N^{-1.75}$ which can be saturated by measuring magnetization on all sites simultaneously. We discuss universal scaling predictions of the estimation precision offered by such observables, both at zero and finite temperatures, and support them with numerical simulations in the model. We provide an experimental proposal of realization of the considered model via mapping the system to ultracold bosons in periodically shaken optical lattice. We explicitly derive that the Heisenberg limit is recovered when time needed for preparation of quantum states involved is taken into account.

PACS numbers: 03.67.Lx, 42.50.Dv

I. INTRODUCTION

At the center of quantum metrology [1–4] lays the concept of estimation of a small external parameter with the help of a quantum procedure. The main idea is to engineer a family of quantum states depending strongly on that parameter in the sense that a small difference in the parameter value makes the states significantly different from each other. The relevant quantifier of a distance between quantum states is the quantum fidelity [5]

$$\mathcal{F}(\hat{\rho}, \hat{\sigma}) = \text{Tr} \left(\sqrt{\sqrt{\hat{\rho}} \hat{\sigma} \sqrt{\hat{\rho}}} \right), \quad (1)$$

where density operators $\hat{\rho}$ and $\hat{\sigma}$ describe the states being compared.

Now consider a family of quantum states $\hat{\rho}(\lambda)$ controlled by a parameter λ and let δ_λ be a small shift of the parameter that we want to estimate. An ultimate

bound on the accuracy of any estimate one may make on the unknown δ_λ is set by the quantum Fisher information (QFI) [3, 6]

$$G(\lambda) = -4 \left. \partial^2 \mathcal{F}(\hat{\rho}(\lambda), \hat{\rho}(\lambda + \delta_\lambda)) / \partial \delta_\lambda^2 \right|_{\delta_\lambda=0}. \quad (2)$$

Indeed, in order to identify δ_λ one has to measure some observable \hat{A} , called an estimator. The precision it offers is quantified by the error propagation formula given by the inverse of signal-to-noise ratio

$$\Delta_{\delta_\lambda}(\hat{A}, \lambda) = \frac{\sqrt{\langle \hat{A}^2 \rangle_{\rho(\lambda)} - \langle \hat{A} \rangle_{\rho(\lambda)}^2}}{\left| \frac{\partial \langle \hat{A} \rangle_{\rho(\lambda + \delta_\lambda)}}{\partial \delta_\lambda} \right|_{\delta_\lambda=0}}. \quad (3)$$

The ultimate lower bound for the uncertainty of estimation of the small deviation δ_λ is set by the quantum Cramer-Rao bound [3],

$$\Delta_{\delta_\lambda}(\hat{A}, \lambda) \geq G(\lambda)^{-1/2}, \quad (4)$$

that is independent of the observable \hat{A} and determined by the QFI. In principle, the above bound would be

* marek.rams@uj.edu.pl

† pawel@mif.pg.gda.pl

‡ jakub.zakrzewski@uj.edu.pl

saturated by some special observable \hat{A} , called symmetric logarithmic derivative operator, satisfying $2\frac{\partial\hat{\rho}(\lambda)}{\partial\lambda} = \hat{A}\hat{\rho}(\lambda) + \hat{\rho}(\lambda)\hat{A}$. In practice, however, an identification of an appropriate symmetric logarithmic derivative operator is a formidable task in itself. We shall show that for a quite general class of systems a possible alternative yielding in some limits at least a correct scaling with the system size exists.

There are basically two different scenarios discussed in the literature on how to introduce the dependence of the state on the parameter $\delta\lambda$. In the first approach [7–9] the state is rotated by some Hamiltonian and then the estimator observable \hat{A} is measured – providing the accuracy that is determined by the error propagation formula. Let us call it a rotation scenario.

In principle, with many-body interacting Hamiltonian the corresponding Fisher information could have implied the error vanishing exponentially with N [10]. It has been proven, however, that when the Hamiltonian is composed only of local on-site (or one-body - see e.g. [11]) terms \hat{h}_n , i.e.

$$\hat{H} = \lambda\hat{H}_1 = \lambda\sum_{n=1}^N\hat{h}_n, \quad (5)$$

then at most $G^{-1/2} \sim N^{-1}$. Such a scaling is referred to as the Heisenberg limit and should be contrasted with the classical type of behavior where $G^{-1/2} \sim N^{-1/2}$, i.e. the shot noise limit. It has been argued that adding to the above Hamiltonian other interactions – not coupled to λ – cannot improve the scaling beyond the Heisenberg limit [11–16]. Furthermore, let us mention that the final formula is quite sensitive to a local noise and because of that one basically always ends up with the classical scaling for large enough N [17].

More precisely, bringing the time of the evolution explicitly into the picture, for the Hamiltonian of the form

$$\hat{H} = \hat{H}_0 + \lambda\hat{H}_1, \quad (6)$$

it has been proven that [11],

$$G^{-1/2} \geq \frac{1}{t\|\hat{H}_1\|}. \quad (7)$$

Above, t is the time of the evolution and $\|\hat{H}_1\|$ is the norm of the operator coupled to $\delta\lambda$. Most importantly, as the time factor might be experimentally limited, the focus usually is on the scaling of the norm only. The above bound holds for any initial state. Saturating it, if at all possible in the general case (even only in the limit of short times), usually requires considering highly entangled GHZ-like probe states.

When the Hamiltonian \hat{H}_1 above includes k -body terms, the possible scaling shifts to $G^{-1/2} \sim N^{-k}$ [11], provided that all possible k -body subsets are present in \hat{H}_1 to contribute to the norm in Eq. (7). In principle, this might allow to go beyond the Heisenberg limit for $k \geq 2$.

Such democratic couplings are, however, difficult to create in Nature. Recently, those results were extended to describe both open and noisy systems [18–22].

The rotation scenario serves also as a powerful entanglement detector [23, 24] which can detect a vanishing fraction of entanglement [25] or even bound entanglement [26] with scaling close to the Heisenberg limit. Entanglement detection method has recently found a new application in the proposal to extract the Fisher information from a dynamical susceptibility of the thermal input state [27] (see also [28]), which is measurable, for instance, by means of Bragg spectroscopy [29, 30]. Recently, the pure state metrology in the spirit of the rotation scenario has been reformulated in terms of the Loschmidt echo [31, 32]. Let us also mention that one can consider Fisher information as a detector of non-equilibrium phase transitions [33, 34] or for multipartite entanglement questions [35]. For a review of quantum enhanced measurements without entanglement see [36].

Having all the above in mind, one immediately recalls the second approach that connects estimation problem to the concept of criticality [37–45]. In that approach one focuses on the situation where the dependence of the state on λ has a completely different origin. The state $|\Psi(\lambda)\rangle$ is the ground state of the Hamiltonian depending on the parameter λ , which exhibits criticality at some critical point λ_c . The essence of this approach is an observation that in the vicinity of the critical point the ground states overlap becomes drastically sensitive to small change of λ . Clearly, this sensitivity is again quantified by QFI.

In the context of ground state fidelity (or more generally for the thermal states) it is customary to introduce fidelity susceptibility $\chi_F(\lambda)$. For sufficiently small $\delta\lambda$, in a finite system, one has

$$\mathcal{F}(\hat{\rho}(\lambda), \hat{\rho}(\lambda + \delta\lambda)) = 1 - \frac{1}{2}\chi_F(\lambda)\delta\lambda^2 + O(\delta\lambda^3). \quad (8)$$

Fidelity susceptibility and QFI are directly proportional to the Bures distance between density matrices at slightly differing values of λ [40, 46] and $G(\lambda) = 4\chi_F(\lambda)$.

Interestingly, it has been observed in this case that for Hamiltonian (6), criticality can boost QFI to $G^{-1/2} \sim N^{-l}$ with $2 < l < 3$, see [47–49], leading to an apparent super-Heisenberg scaling. There seems to exist a clear contradiction with the rotation scenario. Can these two pictures be reconciled? This is the main aim of the present work – we solve this super-Heisenberg puzzle. We show that the overlap measurement contains an additional ingredient, namely the time it takes to transform one ground state into another one at a slightly different parameter value. This may be translated into the additional N -power scaling of time in the vicinity of the critical point if one assumes adiabatic dynamics, which is a necessity if we are to compare ground states. This allows us to reconcile the two approaches to quantum metrology.

The rest of the article is organized as follows. In Sec. II we define and discuss basic properties of fidelity and fidelity susceptibility, the main tools of the analysis that

follow. Sec. III contains the main results of our work. Using finite size scaling hypothesis based on the renormalisation group approach, a well established tool in the treatment of quantum criticality, we derive the scaling of precision offered by the most natural observables coupled to the perturbation. In the adiabatic limit they can saturate the ultimate scaling set by QFI. Most importantly, we also bring the time directly into the picture and discuss the appropriate time scale necessary to recover the adiabatic dynamics at the critical point and reach the above-mentioned scalings. By factoring out the evolution time we illustrate that the ground state approach naturally satisfies the Heisenberg limit as it is understood in the rotational scenario. The apparent super-Heisenberg scalings are recovered in the limit of sufficiently long evolution times and can be understood as the ultimate limit of precision which can be obtained within this approach (whatever the time is). Using a critical ground state as a probe state, nevertheless, might allow to break the shot-noise limit due to strong correlations/entanglement in such a state.

The general theory is illustrated on a particular example in Sec. IV. We discuss the ferromagnetic Heisenberg spin chain where the parameter to be estimated is a small external magnetic field. This model provides a minimal entanglement model in a sense that H_1 is separable while H_0 involves only 2-body (nearest neighbors) terms. Here we test the universal scaling of the error propagation formula for those natural observables against numerical data in the immediate vicinity of the critical point of the model. In particular, we obtain in this model $G^{-1/2}(\lambda_c) \sim N^{-1.75}$ with λ_c being the parameter value at the critical point. Moreover, unlike in the standard, rotation-based metrology, the most natural, strictly local and parameter independent estimator, namely the single-site magnetization, is enough to go beyond the apparent Heisenberg limit by reaching $N^{-1.5}$. We also show that the operator which measures the magnetization on all sites simultaneously scales in the same way as the optimal one. We should point out that finding an analytical form of the optimal operator in many-body system is typically a daunting challenge, see e.g. [39, 40]. With all these interesting properties, when a time factor is properly taken into account (i.e. the time needed to adiabatically transfer a ground state into another ground state at different value of the parameter) we recover the Heisenberg limit.

The possible realization of this model in cold atom optical lattice setting is given in Sec. VII. We found it appropriate to first extend the discussion from smooth adiabatic quench to the instantaneous one, i.e. the Loschmidt echo, arguing that similar universal behavior can be observed also in that case. This is discussed in Sec. V. In Sec. VI we consider the robustness of the observed features, i.e. we consider the situation detuned from criticality as well as the impact of finite temperature. We conclude in Sec. VIII. Finally, in the Appendix A we discuss a universal estimator-type measurement in the paradigm where the original reference state and the spe-

cific quadratic interactions are accessible.

II. BASICS OF FIDELITY SUSCEPTIBILITY

Consider the quantum system depending on a parameter λ , the value of which we shall try to estimate. For the ground state $|\Psi(\lambda)\rangle$ of the Hamiltonian $\hat{H}(\lambda)$ the fidelity defined in Eq. (1) simplifies as

$$\mathcal{F} = |\langle \Psi(\lambda) | \Psi(\lambda + \delta\lambda) \rangle|. \quad (9)$$

It is intuitively clear that fidelity may be significantly below unity, or alternatively that $\chi_F(\lambda)$ (compare Eq. (8)) is large, when the properties of the system change significantly with λ . Then the measurement of some observable might lead to an accurate determination of λ . Clearly, when the system undergoes the quantum phase transition its properties change dramatically, that is why the maxima of $\chi_F(\lambda)$ (for a finite system) or its divergences (in the thermodynamic limit) signal the location of the quantum critical point [37]. Obviously, for Eq. (8) to hold we have to consider a finite system and sufficiently small $\delta\lambda$ – otherwise higher terms in that expansion are non-negligible and one should be considering $\log \mathcal{F}$ which becomes an extensive quantity in that limit [50, 51].

It has been shown that the universal information can be extracted from the behavior of fidelity susceptibility in the vicinity of the critical point [52–55]. To that end, and in order to relate directly to the rotational scenario in Eqs. (5–7), we consider the Hamiltonian

$$\hat{H}(\lambda) = \hat{H}_0 + \lambda \hat{H}_1 = \hat{H}_0 + \lambda \sum_n \hat{h}_n, \quad (10)$$

specifying it to be in a broad class of systems consisting of $N = L^d$ spins in d spatial dimensions which has a continuous critical point at λ_c . The general concept and scaling analysis [56–58] naturally applies also to systems of fermions and bosons. The perturbation coupled to λ in Eq. (10) consists of local on-site terms, note however that the same would hold for \hat{h}_n having support on a couple of neighboring sites. \hat{H}_1 is a relevant renormalisation group perturbation which drives the transition and we assume that it has a well defined scaling dimension. The divergence of the correlation length in the vicinity of the critical point, $\xi \sim |\lambda - \lambda_c|^{-\nu}$, specifies the critical exponent ν .

The universal part of the fidelity susceptibility at the critical point is expected to scale as [53–55]

$$G(\lambda_c)^{1/2} \sim \chi_F(\lambda_c)^{1/2} \sim N^{1/d\nu}. \quad (11)$$

One may also look at $\chi_F(\lambda)$ away from the critical point where the expected scaling reads

$$G(\lambda)^{1/2} \sim \chi_F(\lambda)^{1/2} \sim N^{1/2} |\lambda - \lambda_c|^{d\nu/2-1}. \quad (12)$$

The above universal contributions dominate the behavior of fidelity susceptibility when $d\nu < 2$ so that non-universal, system-specific corrections remain subleading [55, 59].

As a consequence, a realization of a physical system with small ν can lead to a hyper-sensitive estimation of λ . The standard and often considered, exactly solvable one-dimensional spin Ising chain where λ corresponds to the transverse field exhibits the critical point with $\nu = 1$, resulting in $\chi_F(\lambda_c)^{1/2} \sim N$ [40, 60, 61]. In the following we propose a physical realization of another spin system leading to much smaller value of $d\nu < 1$. This provides a more intriguing example of a system which exhibits extreme sensitivity when λ is varied across the critical point, and, on the first sight, might seem to break the Heisenberg limit.

III. METROLOGY AT THE CRITICAL POINT

In this section, we employ the adiabatic theorem to argue how slowly the parameter λ has to change for the system to be able to adjust to it and follow instantaneous ground state. At the critical point this results in a time factor which scales as a power law with the system size. More generally, we show that the time dependence of QFI satisfies the bound where the time factorizes and the remaining scaling with N can exceed the shot noise limit due to strong correlations in the critical ground state. It is however consistent with the Heisenberg limit in Eq. (7). As such we reconcile this approach with the rotational scenario. On the other hand, using finite size scaling analysis we argue that in the adiabatic regime the most natural observables, corresponding to part of the Hamiltonian coupled to λ , offer the same scaling of the error propagation formula as promised by the QFI.

A. Characteristic time scale

First, we estimate the rate of changes of λ which is needed for the system to stay in the instantaneous ground state. We assume that

$$\delta_\lambda(t') = t'/\tau_Q = \frac{t'}{t}\delta_\lambda, \quad (13)$$

for $t' \in [0, t]$, where t is the total time of the evolution, $\delta_\lambda(t) = \delta_\lambda$, and $\tau_Q = t/\delta_\lambda$ is the quench rate. In order to estimate this rate we have to know the behavior of the energy gap at the critical point. For a continuous critical point this gap is expected to scale as $\Delta E \sim L^{-z}$ which introduces the critical exponent z . We also need to estimate the width of the region of λ 's for which the gap is close to its minimal value. Standard finite size argument gives $\Gamma \sim L^{-1/\nu}$. It follows from the general heuristics that in the finite system the gap would be comparable with its minimum when $L \sim \xi(\lambda) \sim |\lambda - \lambda_c|^{-\nu} = \Gamma^{-\nu}$. Now, the adiabatic conditions reads $\Gamma\Delta E \gg 1/\tau_Q$, see e.g. [62]. This is equivalent to

$$\tau_Q \gg L^{\frac{z\nu+1}{\nu}} = N^{\frac{z\nu+1}{d\nu}}. \quad (14)$$

The same estimate of the relevant quench rate is obtained from the application of Kibble-Zurek argument [63–65]. The latter predicts the density of defects excited during the slow quench across the critical point. The adiabatic dynamics corresponds, in that case, to the extreme limit when no defects are created in a finite system.

In order to induce the change of the parameter $\delta_\lambda \sim N^{-1/d\nu}$ which, according to Eq. (11), can possibly be observed, the time must scale at least as

$$\hat{t} \sim \tau_Q \delta_\lambda \sim N^{z/d}. \quad (15)$$

Otherwise, Eq. (15) simply represents the characteristic time scale at the critical point, given by the inverse of the energy gap in the finite system. This means that this time scale would naturally be relevant also beyond the scheme assuming adiabatic evolution and the ground-state overlap. We further elaborate on this point in Sec. V where we briefly discuss how a small instantaneous quench and Loschmidt echo naturally fits into the general picture discussed here.

We can now bringing those scalings together. The bound in Eq. (7) applied to the ground-state fidelity scenario would then read

$$N^{-1/d\nu} \sim G(\lambda_c)^{-1/2} \geq 1/\hat{t} \|\hat{H}_1\| \sim N^{-z/d-1}, \quad (16)$$

note that $\|\hat{H}_1\| \sim N$ which corresponds to the usual Heisenberg factor. In this reasoning we make a straightforward generalization of the argument of [11], valid for time independent systems, to the time dependent adiabatic evolution. In the scaling sense Eq. (16) is equivalent to the condition that $(z+d)\nu \geq 1$.

At this point it is convenient to introduce the scaling dimension of the operator \hat{h} , $[h]$, which describes the rescaling of the operator upon the scale transformation at the critical point. It gives the power-law behavior of the connected correlation function $C(r) = \langle \hat{h}_n \hat{h}_{n+r} \rangle - \langle \hat{h}_n \rangle \langle \hat{h}_{n+r} \rangle \sim r^{-2[h]}$ in the thermodynamic limit. The scaling exponents are not independent but, as we have one relevant operator here, can be typically expressed as a combination of $[h]$, z and d . For instance $\nu = 1/(d+z-[h])$ [58, 66]. As $[h] \geq 0$, this shows that Eq. (16) is indeed consistent within our scaling discussion as $(z+d)\nu \geq 1$ holds.

B. Error propagation formula in the adiabatic limit

Second, we focus on the adiabatic limit, where we discuss the scaling of the error propagation formula of the most natural observables \hat{H}_1 and $\hat{h} = \hat{h}_{N/2}$. We assume \hat{h} to be in the bulk of the system to avoid possibly effects related with the boundaries of the system. It is an exercise in finite size scaling analysis to argue that at the critical point

$$\Delta_{\delta_\lambda}(\hat{H}_1, \lambda_c) \sim N^{-1/d\nu}, \quad (17)$$

$$\Delta_{\delta_\lambda}(\hat{h}_{N/2}, \lambda_c) \sim N^{-1/d\nu+[h]/d}. \quad (18)$$

The first one is saturating the bound provided by the fidelity susceptibility and the second one is close to it for small $[h]$ – see below for the derivation under the assumption that in d -dimensional system the correlation function is vanishing with distance r slower than r^{-d} , and that the hyper-scaling relations hold. Those scalings are closely connected with the important observation that fidelity susceptibility (QFI) can be directly calculated by integrating the dynamic susceptibility of the system to the external driving \hat{H}_1 [27, 52–54, 67].

In order to derive Eqs. (17) and (18) we analyze the scaling of the standard deviation and susceptibility appearing in the error propagation formula in Eq. (3). In the thermodynamic limit the susceptibility $\partial_\lambda \langle \hat{h} \rangle \sim |\lambda - \lambda_c|^{-\theta}$. We assume that the hyper-scaling law holds, i.e. that there are no dangerous irrelevant operators which could modify the scaling hypothesis. In that case $\theta = 1 - [h]\nu$. It is expected to hold for sufficiently low-dimensional system, below the so called upper critical dimension. This is the limit of interest from the perspective of quantum enhanced metrology, as the quantum effects in quantum many-body systems are becoming less important with the growing dimension of the system due to the monogamy of entanglement. In the above, we also assume that $\theta \geq 0$. Otherwise non-universal effects dominate the behavior of susceptibility and effectively $\theta = 0$. Now, the standard finite size scaling argument implies that for a finite system at the critical point $\partial_\lambda \langle \hat{h} \rangle \sim (L^{-1/\nu})^{-\theta} \sim N^{\theta/d\nu}$. Assuming that the standard deviation $\text{std}(\hat{h}) \sim 1$ leads to Eq. (18), where we have used the hyper-scaling relation.

Similarly, the susceptibility $\partial_\lambda \langle \hat{H}_1 \rangle \sim N^{1+\theta/d\nu}$ follows from the scaling for \hat{h} (times factor of N , we additionally assume that possible boundary effects are subleading). It is then enough to estimate the behavior of the standard deviation where we have to take into account the correlator $C(r) \sim r^{-2[h]}$ in the ground state at the critical point. The leading behavior is obtained by integrating the correlation function over the d -dimensional ball of radius L . If $C(r)$ is not vanishing faster than r^{-d} , i.e. for $d - 2[h] > 0$, the integral is dominated by the tail of the correlation function and gives $\sqrt{\langle \hat{H}_1^2 \rangle - \langle \hat{H}_1 \rangle^2} \sim L^{d-[h]} = N^{1-[h]/d}$. Note that the standard deviation corresponds to a structure factor at $k = 0$. Combining the expected scaling of standard deviation and susceptibility, together with the hyper-scaling relation gives Eq. (17).

It is worth to discuss the case of $d - 2[h] \leq 0$ as well. Here, $\sqrt{\langle \hat{H}_1^2 \rangle - \langle \hat{H}_1 \rangle^2} \sim L^{d/2} = N^{1/2}$ and consequently $\Delta_{\delta_\lambda}(\hat{H}_1, \lambda_c) \sim N^{-1/d\nu + [h]/d - 1/2}$. It does not saturate the bound given by QFI and we only see the classical $N^{-1/2}$ improvement over the single-site measurement in Eq. (18). This is, for instance, the case in the often discussed quantum Ising spin chain in the transverse field, $\hat{H} = -\sum_{n=1}^N \sigma_n^x \sigma_{n+1}^x + g \sigma_n^z$. It has a critical point for $g_c = 1$ with the exponent $z = 1$. When $\hat{h}_n = \sigma_n^z$ corresponds to the transverse field the scaling dimension

$[h] = 1$, $\nu = 1$, and effectively $\theta = 0$. The error propagation formula for $\hat{H}_1 = \sum_n \sigma_n^z$ was calculated in [43] and does not saturate the scaling of $G^{-1/2}(g_c) \sim N$. It reads $\Delta_{\delta_\lambda}(\hat{H}_1, \lambda_c) \sim (N \log(N))^{-1/2}$ in agreement with the general prediction above. We note that logarithmic corrections to the scaling are typically expected in this case as $\theta = 0$.

C. Consistency with the rotational scenario

The above scalings of the error propagation formula assume adiabatic dynamics and as such would be recovered for long enough evolution times. At this point we bring the time explicitly into the picture. We show that

$$G(\lambda, t)^{1/2} \leq t2\zeta \sqrt{\langle \hat{H}_1^2 \rangle - \langle \hat{H}_1 \rangle^2}. \quad (19)$$

where the standard deviation is calculated in the initial ground state. The factor $\zeta = \frac{1}{t\delta_\lambda} \int_0^t dt' \delta_\lambda(t')$ follows from the evolution profile in Eq. (13). Here $\zeta = 1/2$. Eq. (19) represents the quantum speed limit adjusted to our setting. For a recent review on quantum speed limits, see e.g. Ref. [68].

For a system at the critical point, as discussed in the previous section, this leads to

$$G(\lambda_c, t)^{1/2} \lesssim t2\zeta N^{1-[h]/d}. \quad (20)$$

We assume here that the correlations $C(r) \sim r^{-2[h]}$ do not vanish too quickly and $d > 2[h]$. Obviously, as $[h] \geq 0$, Eq. (20) is within the general bound (valid for any initial state) given by the Heisenberg limit. In this article – and more generally in the ground state fidelity approach – the focus is on the ground state of the critical system and evolution generated by the Hamiltonian slightly perturbed from it. As can be seen in Eq. (20) this allows to go beyond the shot noise limit, $G(\lambda, t) \sim tN^{1/2}$, as a result of strong entanglement of such an initial state and algebraically vanishing $C(r)$.

For the system detuned from criticality, or when $d - 2[h] \leq 0$, the variance in Eq. (19) is not super-extensive and the classical scaling with N is recovered. This would be again the case for the Ising model briefly discussed at the end of previous section. There, for $\hat{h}_n = \sigma_n^z$ corresponding to the transverse direction, $C(r) \sim r^{-2}$ at the critical point.

It is worth to compare this with the rotational scenario, in which case the suitable GHZ-type probe state is usually considered. We would then have $C(r) \sim 1$ and effectively $[h] = 0$, which saturate the scaling of the Heisenberg limit (at least for short times). Interestingly, critical spin Hamiltonian for which GHZ-state is the ground state can be supplied [69, 70].

The scalings in Eqs. (11,17,18) are reached for the evolution times of the order of $\hat{t} \sim N^{z/d}$, Eq. (15). They comprise the ultimate limits of the criticality-based quantum metrology, giving the title of this article a proper meaning.

To derive Eq. (19) we straightforwardly generalized the result of [13–15] to the time-dependent Hamiltonian, with $\delta_\lambda(t')$ e.g. as in Eq. (13). This leads to [71]

$$G(\lambda, t) = 4\zeta^2 t^2 \left(\langle \Psi | \hat{O}_1^2 | \Psi \rangle - \langle \Psi | \hat{O}_1 | \Psi \rangle^2 \right) = 4\zeta^2 t^2 \text{var} \left(\hat{O}_1 \right),$$

where $\hat{O}_1 = \frac{1}{t\delta_\lambda\zeta} \int_0^t dt' \delta_\lambda(t') U(\lambda, t-t')^\dagger \hat{H}_1 U(\lambda, t-t')$ is time averaged operator \hat{H}_1 rotated by $U(\lambda, t) = e^{-it\hat{H}(\lambda)}$ and $|\Psi\rangle$ is the probe state. As variance is convex, we have $G(\lambda, t) \leq 4t^2\zeta^2 \frac{1}{t\delta_\lambda\zeta} \int_0^t dt' \delta_\lambda(t') \text{var} \left(U(\lambda, t-t')^\dagger \hat{H}_1 U(\lambda, t-t') \right)$.

In our setup we consider the initial state which is the ground state of $\hat{H}(\lambda)$, $|\Psi\rangle = |\Psi(\lambda)\rangle$, which leads to Eq. (19).

IV. EXAMPLE: XXZ MODEL IN THE EXTERNAL FIELD

The discussion in the previous section is general and should hold for a broad class of systems exhibiting continuous quantum critical points. In order to illustrate those predictions, in this section we consider the ferromagnetic XXZ spin- $\frac{1}{2}$ spin chain in the external field. The Hamiltonian reads

$$\hat{H}(\lambda) = - \sum_{n=1}^{N-1} (\sigma_n^x \sigma_{n+1}^x + \sigma_n^y \sigma_{n+1}^y + J_z \sigma_n^z \sigma_{n+1}^z) + \lambda \sum_{n=1}^N \sigma_n^x, \quad (21)$$

where we assume open boundary conditions. $N = L$ is the number of spins ($d = 1$) and J_z is an anisotropy parameter. We consider changes induced by the magnetic field λ with other parameters fixed. For $|J_z| \leq 1$ the system has a critical point at $\lambda_c = 0$ with the critical exponent $z = 1$. The exponent ν was calculated in Ref. [72] and for fixed $-1 < J_z < 1$ reads

$$\nu = \frac{2}{4 - \arccos(J_z)/\pi}, \quad (22)$$

which follows from the scaling dimension of the operator σ^x , $[\sigma^x] = \arccos(J_z)/2\pi$. The desired condition of $d\nu < 1$ is satisfied for all values of $|J_z| < 1$.

We note that fidelity susceptibility for quite similar XXZ model was studied e.g. in Refs. [73–75] both at zero and non-zero temperature. There, however, the external magnetic field λ was not present and the shift of parameters was induced by changing the value of J_z . This leads to a qualitatively different type of behavior related with Berezinskii–Kosterlitz–Thouless critical point and in that case the system does not exhibit super-extensive scaling of the fidelity susceptibility.

At the risk of multiplying the notation let us define the following observables

$$\hat{M}_x \equiv \hat{H}_1 = \sum_{n=1}^N \hat{\sigma}_n^x, \quad (23)$$

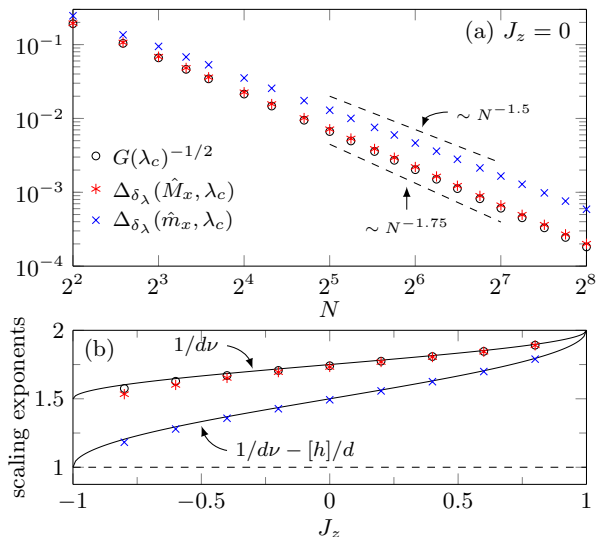


FIG. 1. (Color online) XXZ model in the external field, Eq. (21). (a) Scaling of the error propagation formula for operators \hat{M}_x and \hat{m}_x , and the ultimate bound given by inverse of QFI, as a function of the system size. The error propagation formula for \hat{M}_x closely follows the ultimate bound. Dashed lines indicate the slopes corresponding to the expected scaling and serve as guidance for an eye. The fits give $G(\lambda_c)^{-1/2} \sim N^{-1.74}$, $\Delta_{\delta_\lambda}(\hat{M}_x, \lambda_c) \sim N^{-1.73}$ and $\Delta_{\delta_\lambda}(\hat{m}_x, \lambda_c) \sim N^{-1.49}$, where the expected exponents are 1.75, 1.75 and 1.5, respectively. Here, $J_z = 0$ and the fits were done for $N = 128 \div 256$ [76]. (b) In the considered model the scaling exponents in Eqs. (11,17,18) depend continuously on the value of parameter J_z , following Eq. (22). We compare those predictions with numerical results obtained similarly as in panel (a). The exponent associated with the standard Heisenberg limit is marked with the dashed line for comparison. Its apparent breaking is the main subject of this article.

which corresponds to the simultaneous measurement of magnetization on all sites, and

$$\hat{m}_x \equiv \hat{h}_{N/2} = \hat{\sigma}_{N/2}^x, \quad (24)$$

i.e. the on-site magnetization in the center of the system.

In Fig. 1 we calculate both QFI and the error propagation formula for \hat{M}_x and \hat{m}_x in the adiabatic limit. We numerically verify that the scaling relations in Eqs. (11), (17) and (18) indeed hold in our model. Most importantly, it can be seen that the very natural operator \hat{M}_x practically reproduces the apparent super-Heisenberg scaling allowed by QFI. Moreover, while on-site magnetization in the bulk, \hat{m}_x , grows slower with the system size than the ultimate bound, it is still well in the apparent super-Heisenberg regime. For instance, Eqs. (17,18,22) imply that for $J_z = 0$ we expect $\Delta_{\delta_\lambda}(\hat{M}_x, \lambda_c) \sim N^{-7/4}$ and $\Delta_{\delta_\lambda}(\hat{m}_x, \lambda_c) \sim N^{-3/2}$. This is in excellent agreement with the numerical results presented in panel (a) of Fig. 1. The exponents for other values of parameter J_z , both theoretical predictions and the values fitted from

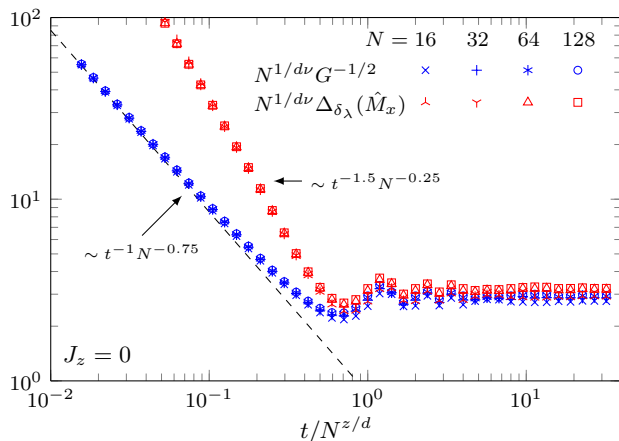


FIG. 2. (Color online) Time dependence of QFI at the critical point in the XXZ model. Results from a small external magnetic field change as in Eq. (13). The time is rescaled by the system size according to (15). QFI (blue symbols) is rescaled corresponding to the adiabatic limit given by Eq. (11). Here, for $J_z = 0$, $z/d = 1$ and $d\nu = 4/7$. For evolution times $t \gg N^{z/d}$ we recover the adiabatic limit. For short times $G^{1/2} \sim tN^{1-[h]/d}$ which is marked with dashed line. In our case $1 - [h]/d = 3/4$. We also show the time dependence of the precision allowed by \hat{M}_x , as described by the error propagation formula (red symbols). For long time, in the adiabatic limit, it is almost optimal and nearly saturates QFI. For short times it is sub-optimal. In that case $\Delta_{\delta\lambda}(\hat{M}_x, \lambda_c, t) \sim t^{-1.5}N^{-0.25}$ is below the shot noise limit as a function of N , see Eq. (25), a result of strong fluctuation at the critical point.

the numerics, are shown in panel (b).

The above results were obtained assuming that the evolution is adiabatic and the time of the evolution might have been, in principle, infinite. We present the limitations imposed by finite evolution time in Fig. 2. To that end the system was initialized in the ground state at the critical point $\lambda_c = 0$. Subsequently, it was evolved to some infinitesimal $\delta\lambda$ according to Eq. (13), with $\tau_Q = t/\delta\lambda$ set by the total evolution time and $\delta\lambda$. We then use Eq. (1) to calculate QFI as a discrete derivative corresponding to Eq. (2) (for small enough $\delta\lambda$).

We rescale the evolution time with the characteristic time-scale in Eq. (15) and the QFI according to the adiabatic (long time) limit in Eq. (11). As can be seen in Fig. 2 the rescaled data obtained for different system sizes collapse, corroborating the scaling predictions. QFI saturates at its adiabatic limit at the time given by Eq. (15). We obtain similar collapse for other values of the anisotropy parameter J_z (not shown).

The bound on QFI given by Eq. (19) is plotted with the dashed line. The bound is tight in the limit of short times, in which case $G(\lambda_c, t)^{1/2} \sim tN^{3/4}$ for $J_z = 0$ plotted in Fig. 2. This scaling is obviously in full agreement with the Heisenberg limit. Employing the ground state of critical system as a probe allows, however, to go beyond

the shot noise limit.

Finally, in Fig. 2 we show how sensitivity allowed by \hat{M}_x depends on time in our setup. As expected, for long enough times $\Delta_{\delta\lambda}(\hat{M}_x, \lambda_c, t)$ saturates at the adiabatic value, almost saturating the ultimate QFI bound. It is however far from being optimal for short times. In that case for $1 \ll t \ll N^{z/d}$ we can expect [77]

$$\Delta_{\delta\lambda}(\hat{H}_1, \lambda_c, t) \sim t^{-\theta/z\nu} N^{-[h]/d}. \quad (25)$$

For $J_z = 0$ in Fig. 2 this translates into $\Delta_{\delta\lambda}(\hat{M}_x, \lambda_c, t) \sim t^{-3/2}N^{-1/4}$. Such scaling of error propagation formula in the limit of short times follows from the behavior of susceptibility, i.e. denominator in Eq. (3). The susceptibility $\partial_\lambda \langle \hat{H}_1 \rangle \sim Nt^{\theta/z\nu}$ which directly follows from the universal scaling of dynamical susceptibility at the critical [56, 57]. As the standard deviation $\sqrt{\langle \hat{H}_1^2 \rangle - \langle \hat{H}_1 \rangle^2} \sim N^{1-[h]/d}$ is set by the reference initial state, this gives Eq. (25). This derivation demonstrates that in this limit strong fluctuations – corresponding to slowly vanishing correlation $C(r)$ – limit the precision allowed by operator \hat{H}_1 , putting it below the shot noise limit. Conversely, we would be able to recover the short noise limit here for $C(r)$ vanishing faster than r^{-d} (or away from the critical point).

All numerical results presented in this sections were obtained using the toolbox of Matrix Product States (MPS) [78–80]. The time evolution is simulated using time dependent variational principle [80], which projects the Schrödinger equation onto the tangent space of the manifold of the MPS. For our problem we use the 4th order time-dependent Suzuki-Trotter decomposition [81], necessary to split the unitary evolution operator onto parts acting on matrices of MPS associated with individual spins. We check that the results are converged both in the discrete time step and MPS bond dimension.

The natural question is how to produce or emulate the above physical system. Such a spin model may be possibly realized for repulsively interacting ultra-cold bosons in optical lattice potential in a quasi-one-dimensional geometry resulting from tight confinement in the perpendicular directions. The optical lattice potential can be precisely controlled, in particular, it can be shaken laterally [82, 83] that allows to change the system properties. By modulating intensity of laser beams forming the optical lattice its depth can be also modulated periodically [84]. Assuming that both processes occur with the same frequency ω , frequency that is much larger than the tunneling frequency as well as a characteristic frequency due to interactions, one can derive an effective time-averaged Hamiltonian governing the long-time physics as reviewed e.g. in [85–87]. Importantly, we assume, that this frequency (or rather its integer multiple, $\mathcal{N}\omega$) is resonant with $s \rightarrow p$ transition between the lowest s , and the excited, p , band. Such a resonance leads to additional slowly varying terms that affect the effective Hamiltonian obtained after time-averaging.

Consider such a system with unit mean filling. Identifying the proper ground state manifold one may describe the dynamics with an effective spin Hamiltonian. Depending on \mathcal{N} one may realize the effective XXZ Heisenberg model for $\mathcal{N} = 2$, or the model that reduces to the desired XXZ Heisenberg Hamiltonian in the magnetic field in Eq. (21) for $\mathcal{N} = 3$. For the interested readers, we provide the explicit derivation in Section VII while we first show that analogical universal behavior holds for instantaneous quench of the Hamiltonian, i.e. the Loschmidt echo. We discuss as well the possible effects due to an imperfect tuning and a finite temperature.

V. LOSCHMIDT ECHO

In the previous sections, in order to be able to recover the limit of adiabatic evolution, we were considering parameter λ changing smoothly in time as in Eq. (13). For completeness of the discussion we briefly comment that qualitatively similar behavior is obtained in the other extreme limit, namely that of a sudden quench. Such a situation is closer to the original spirit of the rotational scenario where the Hamiltonian generating the evolution is usually time independent. To that end we are again going to initialize the system in the ground state of the initial Hamiltonian, focusing on the critical point as the most interesting regime, and consider evolution generated by the Hamiltonian detuned by δ_λ . Fidelity in Eq. (1) gives directly the so called Loschmidt echo which received significant attention in the literature [88], for instance in the studies of decoherence. Most notably for us, it was shown that the decay of the Loschmidt echo is enhanced at the vicinity of the quantum critical point [89].

We illustrate the time dependence of the QFI calculated in this setting, $G_{LE}(\lambda, t)$, for our XXZ model at the critical point with $J_z = 0$ in Fig. 3. The scaling behavior is similar to the smooth quench shown in Fig. (2). Indeed, the general bound in Eq. (19) directly applies to this case, where now $\delta_\lambda(t) = \delta_\lambda$ and $\zeta = 1$. For very short times the bound is tight [90], which follows from the perturbation theory [91], and at the critical point we again get $G_{LE}^{1/2}(\lambda_c, t) \sim tN^{1-[h]/d}$ (under the assumption that $C(r)$ is not vanishing too quickly) [92, 93]. As we consider evolution of the initial ground state by the Hamiltonian which is slightly detuned from the initial one, it is easy to see that QFI cannot grow unbounded and $G_{LE}^{1/2}(\lambda, t) \leq 2G^{1/2}(\lambda)$. Here $G(\lambda) = 4\chi_F(\lambda)$ corresponds to ground state fidelity. At the critical point the bound is reached at the time scale given by Eq. (15). In opposite to the smooth (adiabatic) scenario, Loschmidt echo displays revivals visible as peaks in Fig. 3, characteristic for the critical point [88]. The operator $\hat{M}_x \equiv \hat{H}_1$ again proves to offer a near optimal precision for long times. For short times the derivation in the previous section and Eq. (25) are expected to similarly hold, as can indeed be seen in Fig. 3.

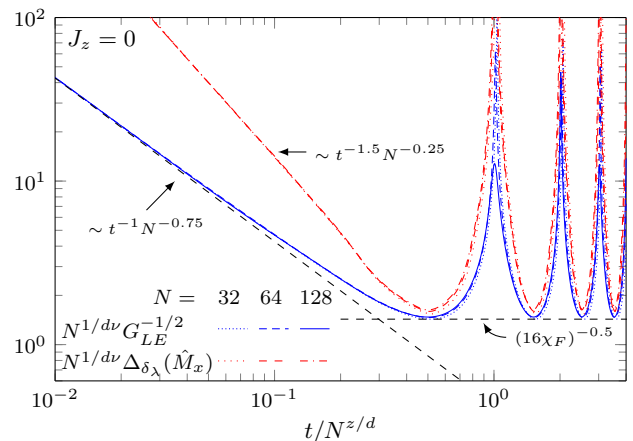


FIG. 3. (Color online) Time dependence of QFI at the critical point in the XXZ model, which results from a small instantaneous shift of the external magnetic field, i.e. the Loschmidt echo. The time is rescaled by the system size according to Eq. (15). The maximal value which can be reached by QFI is bounded by the ground-state fidelity susceptibility (dashed line). We rescale QFI according to Eq. (11). Here, for $J_z = 0$, $z/d = 1$ and $d\nu = 4/7$. For short times $G^{1/2} \sim tN^{1-[h]/d}$, marked with dashed line, with $1 - [h]/d = 3/4$ in our case. For evolution time $t \sim N^{z/d}$ QFI almost reaches its maximal value and later exhibits periodic revivals characteristic for the Loschmidt echo. We also show the time dependence of the precision allowed by \hat{M}_x (red lines). For long time it is close to optimal, mimicking the behavior of QFI. For short times it is sub-optimal. In that case $\Delta_{\delta_\lambda}(\hat{M}_x, \lambda_c, t) \sim t^{-1.5} N^{-0.25}$ is below the shot noise limit as a function of N , see Eq. (25).

VI. ROBUSTNESS TO DETUNING FROM CRITICALITY

To complete the study of scaling results for the error propagation formula, it is quite natural to ask to what extent such a scaling is relevant in real systems, for example due to a non-perfect tuning to the phase transition point and/or a finite temperature of an experiment. Fortunately, general scaling predictions addressing this issue can be provided and verified by numerical simulations, which we show in this section.

First, when λ is not tuned sufficiently close to the critical point, the fidelity susceptibility depends linearly on N as discussed around Eq. (12). The crossover is expected for $L/\xi \sim L|\lambda - \lambda_c|^\nu \sim 1$, where ξ is the correlation length. This means that in order to obtain an apparent super-Heisenberg scaling, λ should be tuned to the critical point within $|\lambda - \lambda_c| \ll L^{-1/\nu}$. This is also the range of δ_λ which can be observed in this case.

In the opposite limit of $|\lambda - \lambda_c| \gg L^{-1/\nu}$, away from the critical point, the error propagation formula are expected

to scale as

$$\Delta_{\delta_\lambda}(\hat{H}_1, \lambda) \sim N^{-1/2} |\lambda - \lambda_c|^{1-d\nu/2}, \quad (26)$$

$$\Delta_{\delta_\lambda}(\hat{h}, \lambda) \sim N^0 |\lambda - \lambda_c|^{-\theta}. \quad (27)$$

The derivation is analogical as in Sec. III. The susceptibility $\partial_\lambda \langle \hat{h} \rangle \sim |\lambda - \lambda_c|^{-\theta}$, together with $\text{std}(\hat{h}) \sim 1$, trivially gives the second of the above relations. For the first one, the standard scaling argument estimates the standard deviation (or a static structure factor) as $\sqrt{\langle \hat{H}_1^2 \rangle - \langle \hat{H}_1 \rangle^2} \sim N^{1/2} \xi^{d/2-[h]} \sim N^{1/2} |\lambda - \lambda_c|^{-\nu d/2+\nu[h]}$, where the correlations are approximately algebraic $\sim r^{-2[h]}$ up to a distance given by the correlation length ξ . Similarly as in Sec. III, we assume here that the algebraic part of the correlation function is vanishing slower than r^{-d} . Otherwise long-distance behavior contributes subleadingly to the standard deviation. Finally, combining this with the susceptibility $\partial_\lambda \langle \hat{H}_1 \rangle \sim N |\lambda - \lambda_c|^{-\theta}$, together with the hyper-scaling relation for θ , gives Eq. (26).

In Figure 4 we numerically verify those scaling predictions for $J_z = 0$ in XXZ model in Eq. (21). While away from the critical point the accuracy allowed by $m_x \equiv \hat{h} = \sigma_{N/2}^x$ becomes significantly worse than the optimal one, the accuracy of $\hat{M}_x \equiv \hat{H}_1 = \sum_n \sigma_n^x$ closely follows the ultimate bound set by QFI. It is worth pointing out that even though we have classical $N^{-1/2}$ scaling in this limit, being in the vicinity of the critical point significantly improves the prefactor as in general, for $d\nu < 2$, $|\lambda - \lambda_c|^{1-d\nu/2} \ll 1$. Similarly as discussed in the previous sections for the critical point, this enhancement comes at a price of suitably longer evolution times. Here, however, the characteristic time scale $\hat{t} \sim \xi^z \sim |\lambda - \lambda_c|^{-z\nu}$ is independent of N .

Second, the pure state idealization discussed so far cannot be fully realized due to the external noise, including the thermal one. Here, for simplicity, we consider the situation where the temperature T is finite but $\lambda = \lambda_c$ is exactly tuned to the critical point. As the finite-size energy gap at the critical point scales as L^{-z} , one expects an apparent super-Heisenberg behavior to hold for $T \ll L^{-z}$.

In the opposite limit of $T \gg L^{-z}$ we recover the classical behavior. We expect

$$\Delta_{\delta_\lambda}(\hat{H}_1, \lambda_c, T) \sim N^{-1/2} T^{(1-d\nu/2)/z\nu}, \quad (28)$$

$$\Delta_{\delta_\lambda}(\hat{h}, \lambda_c, T) \sim N^0 T^{-\theta/z\nu}. \quad (29)$$

To that end, in order to simplify the analysis, we assume that there is no line of thermal phase transitions terminating at the quantum critical point which could alter the behavior and we employ simple scaling analysis, see e.g. [58]. This is the case for our exemplary XXZ model and more broadly for one-dimensional systems.

In this case, the susceptibility $\partial_\lambda \langle \hat{h} \rangle \sim T^{-\theta/z\nu}$ leads to the second of the above relations. With the correlation length $\xi_T \sim T^{-1/z}$, the estimation of the standard deviation gives $\sqrt{\langle \hat{H}_1^2 \rangle - \langle \hat{H}_1 \rangle^2} \sim N^{1/2} \xi_T^{-d/2+[h]} \sim$

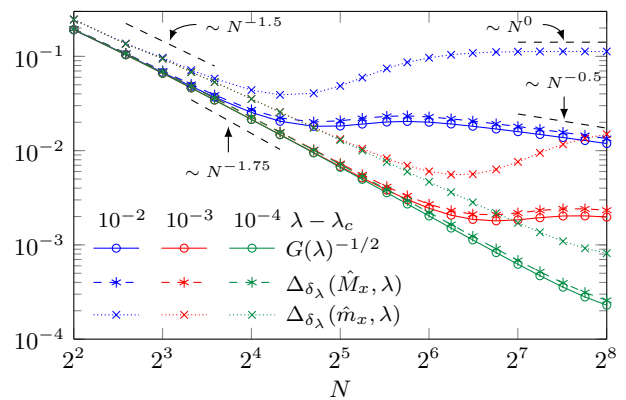


FIG. 4. (Color online) The crossover between different scaling limits when λ is not tuned exactly to the critical point. Results correspond to the adiabatic limit of the evolution. For given deviation $\lambda - \lambda_c$ we recover the apparent super-Heisenberg scaling when N is small enough. When the system size is further increased and $N/\xi^d \sim N|\lambda - \lambda_c|^{d\nu} \gg 1$, $G(\lambda)^{-1/2}$ and $\Delta_{\delta_\lambda}(\hat{M}_x, \lambda)$ have a crossover to the classical $N^{-1/2}$ dependence. On the other hand, $\Delta_{\delta_\lambda}(\hat{m}_x, \lambda)$ saturates and becomes independent on the system size in that limit. Nevertheless, notice that even in this case the prefactors in front of $N^{-1/2(0)}$ are enhanced by the vicinity of the critical point. $\Delta_{\delta_\lambda}(\hat{M}_x, \lambda)$ is closely following the optimal bound set by QFI for all values of the parameters. Dashed lines indicate various scalings and serve as guidance for an eye. Results for the XXZ model in the external field in Eq. (21) with $J_z = 0$.

$N^{1/2} T^{-d/2z+[h]/z}$, where we again assume that the algebraic part of the correlation function is vanishing slower than r^{-d} . Similarly as in the previous case, $\partial_\lambda \langle \hat{H}_1 \rangle \sim N T^{-\theta/z\nu}$, together with the hyper-scaling relation results in Eq. (28).

We illustrate those scaling predictions in our model for $J_z = 0$ in Fig. 5. We employ MPS calculations, where the finite temperature density matrix $\hat{\rho}(\lambda) \sim e^{-\hat{H}(\lambda)/T}$ is expressed as purification and obtained via simulation of the finite system in the imaginary time [78–80]. We again employ time dependent variational principle to that end.

Direct computation of fidelity in Eq. (1) and, in particular, finding the positive square root appearing there is not feasible in the MPS representation. We then follow Ref. [74] and in this case calculate the fidelity defined as $\tilde{F}(\hat{\rho}(\lambda), \hat{\rho}(\lambda + \delta_\lambda)) = \sqrt{\text{Tr} [\hat{\rho}(\lambda)^{1/2} \hat{\rho}(\lambda + \delta_\lambda)^{1/2}]}$. Importantly, as discussed in [74] and derived in [54] if one uses this definition to calculate fidelity susceptibility $\tilde{\chi}_F(\lambda)$ (similarly as in Eq. (8)) then $\tilde{\chi}_F(\lambda) \leq \chi_F(\lambda) \leq 2\tilde{\chi}_F(\lambda)$. This allows us to define $\tilde{G}(\lambda, T) = 8\tilde{\chi}_F(\lambda)$, which sets an upper bound on Fisher information, $\tilde{G}(\lambda, T)/2 < G(\lambda, T) < \tilde{G}(\lambda, T)$, and which we plot in Fig. 5. Those bounds cannot be tightened. Exact diagonalization done for systems of few spins suggests that $G(\lambda, T) \approx \tilde{G}(\lambda, T)/2$ in the limit of small enough N or T . This is also seen in Fig. 5 from comparison to the

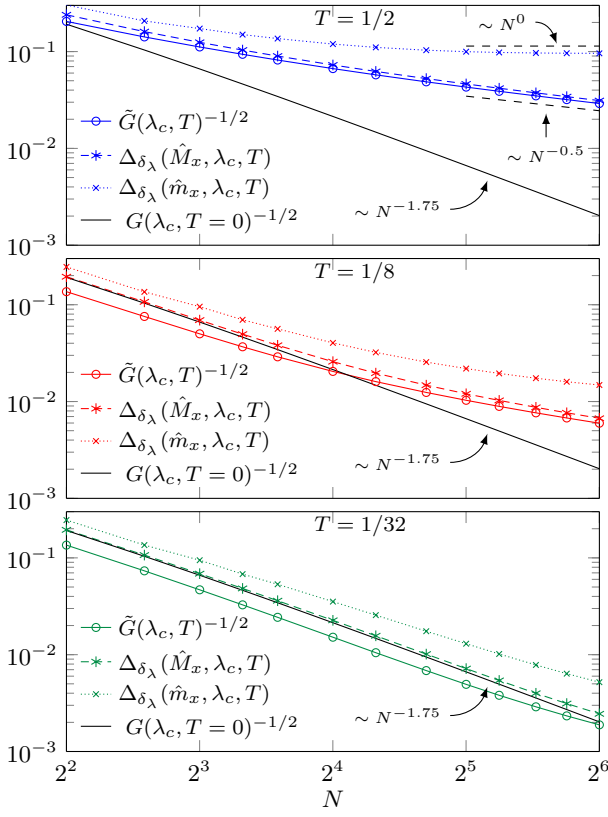


FIG. 5. (Color online) The crossover between different scaling limits when the temperature T is non-zero. Results obtained by comparing states at equilibrium. For given small T we recover the apparent super-Heisenberg scaling when N is small enough, or alternatively for $T \ll N^{-z/d}$. In the opposite limit, when the system size is further increased and $NT^{d/z} \gg 1$, $\tilde{G}(\lambda_c, T)^{-1/2}$ and $\Delta_{\delta_\lambda}(\hat{M}_x, \lambda_c, T)$ have a crossover to the classical $N^{-1/2}$ dependence, however, with the prefactors that are enhanced by the presence of a quantum critical point at $T = 0$. $\Delta_{\delta_\lambda}(\hat{m}_x, \lambda, T)$ saturates and becomes independent on the system size in that limit. Similarly as in Fig. 4, we observe that $\Delta_{\delta_\lambda}(\hat{H}_1, \lambda, T)$ is closely following the optimal bound set by QFI even at non-zero temperatures. $\tilde{G}(\lambda_c, T)^{-1/2}$ plotted here is a lower bound of the (inverse of square root of) the Fisher information, which lies between $\tilde{G}(\lambda_c, T)^{-1/2}$ and $(\tilde{G}(\lambda_c, T)/2)^{-1/2}$ – see text for discussion. Solid lines show the corresponding ultimate bound for $T = 0$ from Fig. 1. Dashed lines indicate various scalings and serve as guidance for an eye. Results for $J_z = 0$.

data for $T = 0$. In the opposite limit of large enough N or T , $G(\lambda, T) \approx \tilde{G}(\lambda, T)$.

In our exemplary XXZ model $z = 1$. Therefore, for $J_z = 0$ and for a large enough system size or temperature, we expect the scalings $\Delta_{\delta_\lambda}(\hat{H}_1, \lambda_c, T) \sim N^{-1/2}T^{1.25}$ and $\Delta_{\delta_\lambda}(\hat{h}, \lambda_c, T) \sim N^0T^{1.5}$, which follow from Eqs. (28,29). By fitting the temperature dependence to the numerical results for $N = 2^6$, i.e. the largest size in Fig. 5, and $T = 0.25 \div 1$ we obtain the exponents equal 1.2 and 1.55, respectively. This is in a reasonable agreement with the

scaling predictions, especially given the numerical limitations. Simulations of the thermal states with MPS is typically much more demanding than the case of pure states, especially in the critical systems, which limits the system sizes which can be simulated here.

It is also worth pointing out that, as can be seen in Fig. 5, $\Delta_{\delta_\lambda}(\hat{H}_1, \lambda_c, T)$ is again closely following the optimal bound set by an inverse of the Fisher information. This is consistent with the scaling of QFI which, similarly to Eqs. (11,12), can be deduced from the scaling dimension of the fidelity susceptibility [52, 53] and standard scaling argument. Those give $\chi_F(\lambda_c, T) \sim NT^{(d\nu-2)/z\nu}$.

At the risk of stating the obvious, it is worth pointing out that the scaling predictions in Eqs. (17,18) and in Eqs. (28,29) correspond to a different order of taking the limits of $T \rightarrow 0$ and $N \rightarrow \infty$ with the smooth crossover when the relevant order is changed.

Finally let us note that the finite temperature approach assumes implicitly a contact of the system with thermal reservoir, i.e., with thermal, Markovian noise. Thus the behavior observed is just the example of the classical scaling recovery for sufficiently large temperature studied in detail recently for a more general case of an arbitrary Markovian noise [22].

VII. COLD-ATOM IMPLEMENTATION

In this section we discuss the possible implementation of the ferromagnetic Heisenberg Hamiltonian (21). We consider the system of ultracold bosons trapped in the quasi 1D optical lattice subject to a periodic driving with frequency fulfilling the resonance condition [94–97]

$$\mathcal{N}\omega = (E_p - E_s) + \mathfrak{d}, \quad (30)$$

where \mathfrak{d} is a small detuning from the transition between levels (bands) with energies E_p and E_s . The dynamics of the system is captured within the two-band Bose-Hubbard model

$$\hat{H}_0 = - \sum_{\langle i,j \rangle} \left(J_s \hat{s}_i^\dagger \hat{s}_j + J_p \hat{p}_i^\dagger \hat{p}_j \right) + \sum_i \left(E_s \hat{n}_i^s + E_p \hat{n}_i^p \right) + \hat{H}_{int},$$

where J_s and J_p are tunnelings in s and p bands, respectively, and the on-site repulsive interactions are accounted for by

$$\hat{H}_{int} = \sum_i \left[\frac{U_{ss}}{2} \hat{n}_i^s (\hat{n}_i^s - 1) + \frac{U_{pp}}{2} \hat{n}_i^p (\hat{n}_i^p - 1) + \frac{U_{sp}}{2} \hat{n}_i^s \hat{n}_i^p \right]. \quad (31)$$

The horizontal lattice shaking modifies the Hamiltonian by the term

$$\begin{aligned} \hat{H}_{hor}(t) = & \cos(\omega t) K \sum_i i (\hat{n}_i^s + \hat{n}_i^p) + \\ & + J \cos(\omega t) \sum_{\langle i,j \rangle} \hat{p}_i^\dagger \hat{s}_j + W \cos(\omega t) \sum_i \hat{p}_i^\dagger \hat{s}_i + h.c., \quad (32) \end{aligned}$$

where the constants K, J, W depend on the amplitude of the periodic driving. The modulation of the intensity of the laser field forming the optical lattice causes the on-site energies to oscillate with amplitudes Δ_s and Δ_p at frequency ω_v .

$$\hat{H}_{ver}(t) = \cos(\omega_v t) \sum_i (\Delta_s \hat{n}_i^s + \Delta_p \hat{n}_i^p). \quad (33)$$

We shall assume $\omega_v = \omega$ in the following for simplicity. The long-time dynamics of the system $H_0 + H_{hor}(t) + H_{ver}(t)$ with $\mathcal{N} = 3$ is described by the effective time-averaged Hamiltonian

$$\begin{aligned} \hat{H}_{eff} = & \sum_i \left(J_{sp}^+ (\hat{p}_i^\dagger \hat{s}_{i+1} + \hat{p}_i \hat{s}_{i+1}^\dagger) + J_{sp}^- (\hat{p}_{i+1}^\dagger \hat{s}_i + \hat{p}_{i+1} \hat{s}_i^\dagger) \right) \\ & + \sum_{\langle i,j \rangle} \left(J_s^{\text{ren}} \hat{s}_i^\dagger \hat{s}_j + J_p^{\text{ren}} \hat{p}_i^\dagger \hat{p}_j \right) + W_{sp} \sum_i (\hat{p}_i^\dagger \hat{s}_i + \hat{p}_i \hat{s}_i^\dagger) + \hat{H}_{int}. \end{aligned} \quad (34)$$

The intra-band tunneling amplitudes are effectively $J_{s,p}^{\text{ren}} = \mathcal{J}_0(K/\omega) J_{s,p}$, where $\mathcal{J}_0(x)$ is a 0-order Bessel function [82, 87, 97]. Similarly, the shaking induced inter-band tunnelings are renormalized by factors dependent on higher order Bessel functions yielding J_{sp}^\pm and W_{sp} [98]. Finally, the energies of the s and p states differ only by the detuning \mathfrak{d} . It is now assumed that $K/\omega = x_0 + \epsilon$ (with $|\epsilon| \ll x_0$) where x_0 is the first zero of \mathcal{J}_0 so that the hopping within the s and p bands is strongly suppressed.

We are interested in the physics of excitations close to the ground state of Eq. (34) with the unit filling in the strongly interacting regime. The Hamiltonian \hat{H}_{eff} , within the second order of perturbation calculus becomes $\hat{H} = -\hat{P}_g \hat{H}_{eff} (\hat{P}_e \hat{H}_{eff} \hat{P}_e - E)^{-1} \hat{H}_{eff} \hat{P}_g$, where \hat{P}_g projects on the subspace of singly occupied states and $\hat{P}_e = 1 - \hat{P}_g$. The condition $\hat{n}_i^s + \hat{n}_i^p = 1$, which holds in the low energy subspace, enables one to define a spin 1/2 degree of freedom at each lattice site leading to Hamiltonian (21) with $\lambda \propto W_{sp} \propto ((\Delta_p - \Delta_s)/\omega)^2$ and parameter J_z depending on the values of ϵ and \mathfrak{d} . Then the spin system in Eq. (21) effectively describes the excitations in the Mott space of the both laterally and vertically shaken optical lattice.

VIII. CONCLUSIONS

Let us summarize our findings. We have discussed two approaches to quantum estimation of a parameter, approaches that give seemingly different predictions. This difference becomes apparent close to the critical phase transition points. In the first approach, referred to as a rotation scenario, the system is compared with its copy rotated by the parameter dependent dynamics. The ultimate limit in this case is known as the Heisenberg limit. The second approach relies on the overlap of ground

states of the system at slightly different values of the parameter. Here one may often arrive at an apparent super-Heisenberg scaling close to criticality.

The main result of our work is to provide a unified picture that links these two approaches. The necessary ingredient is an observation that the physical comparison of ground states at different parameter values can be operationally realized in an adiabatic evolution only. Under this assumption we provide an argument that both approaches yield essentially the same scaling, consistent with the Heisenberg limit when this time factor is taken into account. In effects we obtain a straightforward generalization of the argument of [11–15], valid for time independent systems, to an adiabatic evolution.

Importantly, our finding should hold for a broad class of a quantum many-body systems (in one or more spacial dimensions), with a particular focus on the second-order quantum critical points. As a by product we identify the optimal observable that reveals the optimal scaling in the adiabatic limit - it is identified as a part of the Hamiltonian coupled to the parameter (i.e. H_1 in (10)).

The general result has been confirmed in a detailed study of the ferromagnetic Heisenberg Hamiltonian. On one side it forms a “minimal” Hamiltonian that reveals an apparent super-Heisenberg scaling with global magnetization as the optimal observable. We have shown that this “super-Heisenberg” behavior is quite robust with respect to detuning from the critical point as well as temperature. Yet, as verified in our numerical study, the time needed for measurement of the overlap (i.e. performing the necessary time evolution) leads to the recovery of the Heisenberg scaling in total agreement with the rotation scenario.

The standard metrological approach claims that the scaling may grow with the range of the interaction involving the unknown parameter [10], i.e. super-Heisenberg behavior is in general possible if we replace the one-body operators in Eq. (10) by multiple many-body terms. However, that may reduce the possible gap in the system and therefore affect the time needed to physically realize ground states the fidelity of which is supposed to be measured. The viewpoint developed here is that any super-Heisenberg claim must be accompanied by a careful analysis not only of system size scaling but also the time needed to prepare a given measurement.

Specifically, cold atomic systems offer direct measurements of the fidelity susceptibility *without necessity of the unitary rotation* by means of the Bragg spectroscopy. That may allow to break the “unitary rotation paradigm” although the careful analysis of a specific experiment is needed before giving the definite answer. In particular, high frequency resolution in Bragg spectroscopy and importance of low frequencies for fidelity susceptibility necessitates a sufficiently long time of measurement. The discussion of that point is beyond the scope of the present paper. Similar remarks may be addressed to “swap measurement” (see the appendix A where this idea is developed) that also does not involve “unitary rotation”.

So while we have not provided all the answers leaving some place for future investigations, we believe that we were able at least to understand the apparent discrepancy between the unitary rotation approach and fidelity susceptibility behavior at criticality.

ACKNOWLEDGMENTS

We are grateful to Bogdan Damski and Jacek Dziarmaga for numerous discussions and hints. P. S. and J. Z. acknowledge support by PL-Grid Infrastructure and EU project the EU H2020-FETPROACT-2014 Project QUIC No.641122, while P. H. acknowledges the support of the ERC AdG QOLAPS project. This research has been supported by National Science Centre (Poland) under projects 2011/01/B/ST2/05459 (P.H.), 2015/19/B/ST2/01028 (P.S.), 2016/21/B/ST2/01086 (J.Z.) and 2013/09/B/ST3/00239 (M.M.R.).

Appendix A: An universal quadratic estimator for pure states

Consider an arbitrary Hamiltonian $\hat{H}(\lambda)$ and suppose that we have significant reasons to believe that λ is critical, but for technical reasons it is difficult to prove it. In particular, there is no linear estimator known – like the two observables discussed in the main text – that could provide an accuracy close to the limit of Fisher information scaling. The question is whether there is any way to design an experiment that would allow to circumvent the above difficulty. To answer this affirmatively, we shall provide a simple estimator, quadratic in terms of the interaction involved, which however remains relatively simple and, at least in principle, can be detected with the present state of the art technology of optical lattices.

Let us assume that apart from $|\Psi(\lambda + \delta\lambda)\rangle$, experimentalist can also prepare the state at the critical point $|\Psi(\lambda)\rangle$. Now, it is known that \mathcal{F}^2 – the square of fidelity in Eq. (9) between the two above states – can be detected using the so called universal quantum estimator [99, 100], which is measurable involving at most quadratic interaction among elementary qubits corresponding to the series of independent Hong-Ou-Mandel type measurements [101]. The main idea behind it is to measure the quantity $\text{Tr}(\hat{\rho}\hat{\sigma})$, which is the mean value of the *swap* observable (defined below) jointly measured on the product state $\hat{\rho} \otimes \hat{\sigma}$. The first experiment of this type has been performed relatively long time ago on two copies of the same state of the polarization-entangled photon pairs, which aimed at estimation of Renyi-2 entropy to show that violation of suitable inequality can serve as entanglement

detector [102].

Consider the *swap* operator \hat{S} which by definition acts as $\hat{S}|i\rangle|j\rangle = |j\rangle|i\rangle$ on $\mathcal{H} \otimes \mathcal{H}$. Alternatively, it can be represented as

$$\hat{S} = \hat{\mathbb{1}}_{\mathcal{H}} \otimes \hat{\mathbb{1}}_{\mathcal{H}} - 2\hat{P}^{asym}_{\mathcal{H} \otimes \mathcal{H}}, \quad (\text{A1})$$

where \hat{P}^{asym} is the projector on the antisymmetric subspace of $\mathcal{H} \otimes \mathcal{H}$. Then the obvious observable which measures \mathcal{F}^2 is

$$\hat{A}_{swap} = \hat{S}^{\otimes N} = \hat{\mathbb{1}}_{\mathcal{H}^{\otimes N}} \otimes \hat{\mathbb{1}}_{\mathcal{H}^{\otimes N}} - 2\hat{P}^{asym}_{\mathcal{H}^{\otimes N} \otimes \mathcal{H}^{\otimes N}} \quad (\text{A2})$$

acting on the “quadratic” state $|\Phi\rangle = |\Psi(\lambda)\rangle \otimes |\Psi(\lambda + \delta\lambda)\rangle$ composed of $2N$ elementary subsystems, where each \hat{S} acts on one element of, respectively, first and second pure states. The above measurement corresponds to coupling each elementary subsystem of the first chain of N spins, with the corresponding subsystem of the second chain and performing the measurement by projecting it on the antisymmetric subspace and then multiply the results. This gives the overall results of $+1$ (-1) when the number of successive projections is even (odd).

Now it is an elementary exercise to see that in this case the error propagation formula of Eq. (3) takes the form

$$\Delta_{\delta\lambda}(\hat{A}_{swap}, \lambda) = \frac{1}{\sqrt{2\chi_{\mathcal{F}}(\lambda)}} = \sqrt{\frac{2}{G(\lambda)}}, \quad (\text{A3})$$

where we employ Eq. (8) and $\hat{A}_{swap}^2 = \hat{\mathbb{1}}$. The error propagation formula in Eq. (A3) is then only by a factor of two worse than the best possible linear estimator. Therefore, we got a quadratic estimator that reproduces – up to the constant factor – the scaling in N of the best possible linear one. Note that applying the above procedure to the original unitary perturbation scheme (like in eg. [9, 27, 43]) can not surpass the Heisenberg limit, since the whole scheme may be simulated as a measurement of some new observable on the $|\Psi(\lambda)\rangle$ alone which is known to obey the limit as long as the part of the Hamiltonian with unknown parameter λ is fully local, see [13, 14, 16].

Now the question is: can we employ the above approach for the case of bosonic lattices considered in Sec. VII? Fortunately, the answer is, at least in principle, affirmative. Indeed, very recently it has been shown how to directly perform the measurement of the swap observable on the bosonic lattices [103–106] where the authors designed the beam-splitter type of interaction as a tunneling coupling between two optical lattices, followed by the measurement of the parity of the on-site occupation numbers. This guarantees that the observable in Eq. (A2), which is crucial for the experimental application of the formula (A3) can be directly measured on the optical system with an effective spin Hamiltonian having the critical parameter introduced by lattice shaking.

- [1] C. M. Caves, Phys. Rev. D **23**, 1693 (1981), URL <http://link.aps.org/doi/10.1103/PhysRevD.23.1693>.
- [2] D. J. Wineland, J. J. Bollinger, W. M. Itano, F. L. Moore, and D. J. Heinzen, Phys. Rev. A **46**, R6797 (1992), URL <http://link.aps.org/doi/10.1103/PhysRevA.46.R6797>.
- [3] S. L. Braunstein and C. M. Caves, Phys. Rev. Lett. **72**, 3439 (1994), URL <https://link.aps.org/doi/10.1103/PhysRevLett.72.3439>.
- [4] V. Giovannetti, S. Lloyd, and L. Maccone, Science **306**, 1330 (2004), ISSN 0036-8075, <http://science.sciencemag.org/content/306/5700/1330.full.pdf>, URL <http://science.sciencemag.org/content/306/5700/1330>.
- [5] A. Uhlmann, Reports on Mathematical Physics **9**, 273 (1976), ISSN 0034-4877, URL <http://www.sciencedirect.com/science/article/pii/0034487776900604>.
- [6] M. M. Taddei, B. M. Escher, L. Davidovich, and R. L. de Matos Filho, Phys. Rev. Lett. **110**, 050402 (2013), URL <https://link.aps.org/doi/10.1103/PhysRevLett.110.050402>.
- [7] V. Giovannetti, S. Lloyd, and L. Maccone, Nature Photonics **5**, 222 EP (2011), review Article, URL <http://dx.doi.org/10.1038/nphoton.2011.35>.
- [8] G. Tóth and I. Apellaniz, J. Phys. A **47**, 424006 (2014), URL <http://stacks.iop.org/1751-8121/47/i=42/a=424006>.
- [9] R. Demkowicz-Dobrzanski, M. Jarzyna, and J. Kolodynski, Progress in Optics **60**, 345 (2015), URL <http://www.sciencedirect.com/science/article/pii/S0079663815000049>.
- [10] S. M. Roy and S. L. Braunstein, Phys. Rev. Lett. **100**, 220501 (2008), URL <http://link.aps.org/doi/10.1103/PhysRevLett.100.220501>.
- [11] S. Boixo, S. T. Flammia, C. M. Caves, and J. Geremia, Phys. Rev. Lett. **98**, 090401 (2007), URL <http://link.aps.org/doi/10.1103/PhysRevLett.98.090401>.
- [12] V. Giovannetti, S. Lloyd, and L. Maccone, Phys. Rev. Lett. **96**, 010401 (2006), URL <https://link.aps.org/doi/10.1103/PhysRevLett.96.010401>.
- [13] A. De Pasquale, D. Rossini, P. Facchi, and V. Giovannetti, Phys. Rev. A **88**, 052117 (2013), URL <http://link.aps.org/doi/10.1103/PhysRevA.88.052117>.
- [14] M. Skotiniotis, P. Sekatski, and W. Dür, New Journal of Physics **17**, 073032 (2015), URL <http://stacks.iop.org/1367-2630/17/i=7/a=073032>.
- [15] S. Pang and T. A. Brun, Phys. Rev. A **90**, 022117 (2014), URL <https://link.aps.org/doi/10.1103/PhysRevA.90.022117>.
- [16] J. Fraise and D. Braun, arXiv:1610.05974 (2016).
- [17] R. Demkowicz-Dobrzanski, J. Kolodynski, and M. Guta, Nat. Comm. **3**, 1063 (2012), URL <http://dx.doi.org/10.1038/ncomms2067>.
- [18] S. Alipour, M. Mehboudi, and A. T. Rezakhani, Phys. Rev. Lett. **112**, 120405 (2014), URL <https://link.aps.org/doi/10.1103/PhysRevLett.112.120405>.
- [19] S. Alipour and A. T. Rezakhani, Phys. Rev. A **91**, 042104 (2015), URL <https://link.aps.org/doi/10.1103/PhysRevA.91.042104>.
- [20] A. Chenu, M. Beau, J. Cao, and A. del Campo, Phys. Rev. Lett. **118**, 140403 (2017), URL <https://link.aps.org/doi/10.1103/PhysRevLett.118.140403>.
- [21] M. Beau and A. del Campo, Phys. Rev. Lett. **119**, 010403 (2017), URL <https://link.aps.org/doi/10.1103/PhysRevLett.119.010403>.
- [22] R. Demkowicz-Dobrzański, J. Czajkowski, and P. Sekatski, Phys. Rev. X **7**, 041009 (2017), URL <https://link.aps.org/doi/10.1103/PhysRevX.7.041009>.
- [23] P. Hyllus, W. Laskowski, R. Krischek, C. Schwemmer, W. Wieczorek, H. Weinfurter, L. Pezzé, and A. Smerzi, Phys. Rev. A **85**, 022321 (2012), URL <http://link.aps.org/doi/10.1103/PhysRevA.85.022321>.
- [24] G. Tóth, Phys. Rev. A **85**, 022322 (2012), URL <http://link.aps.org/doi/10.1103/PhysRevA.85.022322>.
- [25] R. Augusiak, J. Kołodyński, A. Streltsov, M. N. Bera, A. Acín, and M. Lewenstein, Phys. Rev. A **94**, 012339 (2016), URL <http://link.aps.org/doi/10.1103/PhysRevA.94.012339>.
- [26] L. Czekaj, A. Przysiężna, M. Horodecki, and P. Horodecki, Phys. Rev. A **92**, 062303 (2015), URL <http://link.aps.org/doi/10.1103/PhysRevA.92.062303>.
- [27] P. Hauke, M. Heyl, L. Tagliacozzo, and P. Zoller, Nat. Phys. **12**, 778 (2016), URL <http://dx.doi.org/10.1038/nphys3700>.
- [28] I. Apellaniz, M. Kleinmann, O. Gühne, and G. Tóth, Phys. Rev. A **95**, 032330 (2017), URL <https://link.aps.org/doi/10.1103/PhysRevA.95.032330>.
- [29] P. T. Ernst, S. Gotze, J. S. Krauser, K. Pyka, D.-S. Luhmann, D. Pfannkuche, and K. Sengstock, Nat Phys **6**, 56 (2010), ISSN 1745-2473, URL <http://dx.doi.org/10.1038/nphys1476>.
- [30] D. Clément, N. Fabbri, L. Fallani, C. Fort, and M. Inguscio, J. Low Temp. Phys. **158**, 5 (2010), URL <http://dx.doi.org/10.1007/s10909-009-0040-7>.
- [31] M. Tsang, Phys. Rev. A **88**, 021801 (2013), URL <https://link.aps.org/doi/10.1103/PhysRevA.88.021801>.
- [32] T. Macri, A. Smerzi, and L. Pezzè, Phys. Rev. A **94**, 010102 (2016), URL <http://link.aps.org/doi/10.1103/PhysRevA.94.010102>.
- [33] U. Marzolino and T. Prosen, Phys. Rev. A **90**, 062130 (2014), URL <http://link.aps.org/doi/10.1103/PhysRevA.90.062130>.
- [34] U. Marzolino and T. Prosen, Phys. Rev. A **93**, 032306 (2016), URL <http://link.aps.org/doi/10.1103/PhysRevA.93.032306>.
- [35] M. A. Rajabpour, Phys. Rev. D **96**, 126007 (2017), URL <https://link.aps.org/doi/10.1103/PhysRevD.96.126007>.
- [36] D. Braun, G. Adesso, F. Benatti, R. Floreanini, U. Marzolino, M. W. Mitchell, and S. Pirandola, ArXiv e-prints (2017), 1701.05152.
- [37] P. Zanardi and N. Paunković, Phys. Rev. E **74**, 031123 (2006), URL <https://link.aps.org/doi/10.1103/PhysRevE.74.031123>.
- [38] W.-L. You, Y.-W. Li, and S.-J. Gu, Phys. Rev. E **76**, 022101 (2007), URL <http://link.aps.org/doi/10.1103/PhysRevE.76.022101>.
- [39] P. Zanardi, M. G. A. Paris, and L. Campos Venuti, Phys. Rev. A **78**, 042105 (2008), URL <http://link.aps.org/doi/10.1103/PhysRevA.78.042105>.

- [40] C. Invernizzi, M. Korbman, L. Campos Venuti, and M. G. A. Paris, Phys. Rev. A **78**, 042106 (2008), URL <http://link.aps.org/doi/10.1103/PhysRevA.78.042106>.
- [41] G. Salvatori, A. Mandarino, and M. G. A. Paris, Phys. Rev. A **90**, 022111 (2014), URL <https://link.aps.org/doi/10.1103/PhysRevA.90.022111>.
- [42] M. Bina, I. Amelio, and M. G. A. Paris, Phys. Rev. E **93**, 052118 (2016), URL <https://link.aps.org/doi/10.1103/PhysRevE.93.052118>.
- [43] W. L. Boyajian, M. Skotiniotis, W. Dür, and B. Kraus, Phys. Rev. A **94**, 062326 (2016), URL <https://link.aps.org/doi/10.1103/PhysRevA.94.062326>.
- [44] M. Mehboudi, L. A. Correa, and A. Sanpera, Phys. Rev. A **94**, 042121 (2016), URL <https://link.aps.org/doi/10.1103/PhysRevA.94.042121>.
- [45] I. Frérot and T. Roscilde, ArXiv e-prints (2017), 1707.08804.
- [46] M. Hübner, Phys. Lett. A **179**, 226 (1993), ISSN 0375-9601, URL <http://www.sciencedirect.com/science/article/pii/037596019390668P>.
- [47] L. Gong and P. Tong, Phys. Rev. B **78**, 115114 (2008), URL <https://link.aps.org/doi/10.1103/PhysRevB.78.115114>.
- [48] S.-J. Gu, H.-M. Kwok, W.-Q. Ning, and H.-Q. Lin, Phys. Rev. B **77**, 245109 (2008), URL <https://link.aps.org/doi/10.1103/PhysRevB.77.245109>.
- [49] S. Greschner, A. K. Kolezhuk, and T. Vekua, Phys. Rev. B **88**, 195101 (2013), URL <https://link.aps.org/doi/10.1103/PhysRevB.88.195101>.
- [50] H. Zhou and J. P. Barjaktarevič, J. Phys. A **41**, 412001 (2008).
- [51] M. M. Rams and B. Damski, Phys. Rev. Lett. **106**, 055701 (2011), URL <https://link.aps.org/doi/10.1103/PhysRevLett.106.055701>.
M. M. Rams and B. Damski, Phys. Rev. A **84**, 032324 (2011), URL <https://link.aps.org/doi/10.1103/PhysRevA.84.032324>.
- [52] L. Campos Venuti and P. Zanardi, Phys. Rev. Lett. **99**, 095701 (2007), URL <https://link.aps.org/doi/10.1103/PhysRevLett.99.095701>.
- [53] D. Schwandt, F. Alet, and S. Capponi, Phys. Rev. Lett. **103**, 170501 (2009), URL <https://link.aps.org/doi/10.1103/PhysRevLett.103.170501>.
- [54] A. F. Albuquerque, F. Alet, C. Sire, and S. Capponi, Phys. Rev. B **81**, 064418 (2010), URL <https://link.aps.org/doi/10.1103/PhysRevB.81.064418>.
- [55] V. Gritsev and A. Polkovnikov, in *Understanding in Quantum Phase Transitions* edited by L. Carr (Taylor & Francis, Boca Raton, 2010); arXiv:0910.3692.
- [56] S. Sachdev, *Quantum Phase Transitions* (Cambridge University Press, Cambridge, U.K., 1999).
- [57] S. L. Sondhi, S. M. Girvin, J. P. Carini, and D. Shahar, Rev. Mod. Phys. **69**, 315 (1997), URL <https://link.aps.org/doi/10.1103/RevModPhys.69.315>.
- [58] M. A. Continentino, *Quantum Scaling in Many-Body Systems* (World Scientific Publishing, Singapore, 2001).
- [59] C. De Grandi, V. Gritsev, and A. Polkovnikov, Phys. Rev. B **81**, 012303 (2010), URL <https://link.aps.org/doi/10.1103/PhysRevB.81.012303>.
C. De Grandi, V. Gritsev, and A. Polkovnikov, Phys. Rev. B **81**, 224301 (2010), URL <https://link.aps.org/doi/10.1103/PhysRevB.81.224301>.
- [60] Y. Chen, Z. D. Wang, Y. Q. Li, and F. C. Zhang, Phys. Rev. B **75**, 195113 (2007), URL <http://link.aps.org/doi/10.1103/PhysRevB.75.195113>.
- [61] B. Damski, Phys. Rev. E **87**, 052131 (2013), URL <https://link.aps.org/doi/10.1103/PhysRevE.87.052131>.
B. Damski and M. M. Rams, Journal of Physics A: Mathematical and Theoretical **47**, 025303 (2014), URL <http://stacks.iop.org/1751-8121/47/i=2/a=025303>.
- [62] S. Knysh, Nature Communications **7**, 12370 (2016).
- [63] W. H. Zurek, U. Dorner, and P. Zoller, Phys. Rev. Lett. **95**, 105701 (2005), URL <https://link.aps.org/doi/10.1103/PhysRevLett.95.105701>.
- [64] J. Dziarmaga, Adv. Phys. **59**, 1063 (2010), URL <http://dx.doi.org/10.1080/00018732.2010.514702>.
- [65] A. Polkovnikov, K. Sengupta, A. Silva, and M. Vengalattore, Rev. Mod. Phys. **83**, 863 (2011), URL <https://link.aps.org/doi/10.1103/RevModPhys.83.863>.
- [66] J. Cardy, *Scaling and renormalization in statistical physics*, vol. 5 (Cambridge university press, 1996).
- [67] W.-L. You, Y.-W. Li, and S.-J. Gu, Phys. Rev. E **76**, 022101 (2007), URL <https://link.aps.org/doi/10.1103/PhysRevE.76.022101>.
- [68] S. Deffner and S. Campbell, Journal of Physics A: Mathematical and Theoretical **50**, 453001 (2017), URL <http://stacks.iop.org/1751-8121/50/i=45/a=453001>.
- [69] Following [70] consider the cluster-Ising spin chain $H_0 = -\sum_n (2\sigma_n^z \sigma_{n+1}^z + \sigma_n^x - \sigma_n^z \sigma_{n+1}^x \sigma_{n+2}^z)$ which is critical and has GHZ state as the ground state. Now, the relevant perturbation aligned with this state is $H_1 = -\sum_n h_n = -\sum_n \sigma_n^z$. In such system $z = 2$ and $[h] = 0$.
- [70] M. M. Wolf, G. Ortiz, F. Verstraete, and J. I. Cirac, Phys. Rev. Lett. **97**, 110403 (2006), URL <https://link.aps.org/doi/10.1103/PhysRevLett.97.110403>.
- [71] See for instance Eqs. (7-9) in Ref. [14]. In Eq. (8) we allow a small change of, say, λ_1 to depend on time.
- [72] I. Affleck and M. Oshikawa, Phys. Rev. B **60**, 1038 (1999), URL <http://link.aps.org/doi/10.1103/PhysRevB.60.1038>.
- [73] L. Campos Venuti and P. Zanardi, Phys. Rev. Lett. **99**, 095701 (2007), URL <http://link.aps.org/doi/10.1103/PhysRevLett.99.095701>.
- [74] J. Sirker, Phys. Rev. Lett. **105**, 117203 (2010), URL <https://link.aps.org/doi/10.1103/PhysRevLett.105.117203>.
- [75] G. Sun, A. K. Kolezhuk, and T. Vekua, Phys. Rev. B **91**, 014418 (2015), URL <http://link.aps.org/doi/10.1103/PhysRevB.91.014418>.
- [76] Experienced reader may wonder that for odd N the ground state is exactly degenerate at the critical point $\lambda_c = 0$, which leads to singularity in χ_F if one uses Eq. (9) directly. For simplicity of the discussion, we use even N in the numerics.
- [77] In the perturbative regime of $t \ll 1$ it is easy to see that $\Delta_{\delta_x}(\hat{H}_1, \lambda_c, t) \sim t^{-2}$. Such region is not shown in Fig. 2.
- [78] F. Verstraete, V. Murg, and J. I. Cirac, Advances in Physics **57**, 143 (2008), URL <http://dx.doi.org/10.1080/14789940801912366>.
- [79] U. Schollwock, Annals of Physics **326**, 96 (2011), ISSN 0003-4916, URL <http://www.sciencedirect.com/science/article/pii/S0003491610001752>.
- [80] J. Haegeman, J. I. Cirac, T. J. Osborne, I. Pižorn, H. Verschelde, and F. Verstraete, Phys. Rev. Lett.

- 107, 070601 (2011), URL <http://link.aps.org/doi/10.1103/PhysRevLett.107.070601>.
- J. Haegeman, C. Lubich, I. Oseledets, B. Vandereycken, and F. Verstraete, Phys. Rev. B **94**, 165116 (2016), URL <http://link.aps.org/doi/10.1103/PhysRevB.94.165116>.
- [81] M. Suzuki, Proceedings of the Japan Academy, Series B **69**, 161 (1993), URL <https://doi.org/10.2183/pjab.69.161>.
- N. Hatano and M. Suzuki, in *Quantum annealing and other optimization methods* (Springer, 2005), pp. 37–68.
- [82] A. Eckardt, C. Weiss, and M. Holthaus, Phys. Rev. Lett. **95**, 260404 (2005), URL <http://link.aps.org/doi/10.1103/PhysRevLett.95.260404>.
- [83] A. Eckardt, P. Hauke, P. Soltan-Panahi, C. Becker, K. Sengstock, and M. Lewenstein, EPL (Europhysics Letters) **89**, 10010 (2010), URL <http://stacks.iop.org/0295-5075/89/i=1/a=10010>.
- [84] M. Łącki and J. Zakrzewski, Phys. Rev. Lett. **110**, 065301 (2013), URL <http://link.aps.org/doi/10.1103/PhysRevLett.110.065301>.
- [85] N. Goldman and J. Dalibard, Phys. Rev. X **4**, 031027 (2014), URL <http://link.aps.org/doi/10.1103/PhysRevX.4.031027>.
- [86] M. Bukov, L. D'Alessio, and A. Polkovnikov, Advances in Physics **64**, 139 (2015), URL <https://doi.org/10.1080/00018732.2015.1055918>.
- [87] A. Eckardt and E. Anisimovas, New J. Phys. **17**, 093039 (2015), URL <http://stacks.iop.org/1367-2630/17/i=9/a=093039>.
- [88] A. Dutta, G. Aeppli, B. K. Chakrabarti, U. Divakaran, T. F. Rosenbaum, and D. Sen, *Quantum Phase Transitions in Transverse Field Spin Models: From Statistical Physics to Quantum Information* (Cambridge University Press, Cambridge, 2015).
- [89] H. T. Quan, Z. Song, X. F. Liu, P. Zanardi, and C. P. Sun, Phys. Rev. Lett. **96**, 140604 (2006), URL <https://link.aps.org/doi/10.1103/PhysRevLett.96.140604>.
- [90] A. Peres, Phys. Rev. A **30**, 1610 (1984), URL <https://link.aps.org/doi/10.1103/PhysRevA.30.1610>.
- [91] Note that here the scaling remains tight also beyond the perturbative regime of very short times.
- [92] L. Campos Venuti and P. Zanardi, Phys. Rev. A **81**, 022113 (2010), URL <https://link.aps.org/doi/10.1103/PhysRevA.81.022113>.
- [93] V. Mukherjee, S. Sharma, and A. Dutta, Phys. Rev. B **86**, 020301 (2012), URL <https://link.aps.org/doi/10.1103/PhysRevB.86.020301>.
- [94] C. Sträter and A. Eckardt, Phys. Rev. A **91**, 053602 (2015), URL <https://link.aps.org/doi/10.1103/PhysRevA.91.053602>.
- [95] A. Przysiężna, O. Dutta, and J. Zakrzewski, New Journal of Physics **17**, 013018 (2015), URL <http://stacks.iop.org/1367-2630/17/i=1/a=013018>.
- [96] A. Dutta, A. Przysiężna, and J. Zakrzewski, Scientific Reports **5**, 11060 EP (2015), article, URL <http://dx.doi.org/10.1038/srep11060>.
- [97] A. Eckardt, Rev. Mod. Phys. **89**, 011004 (2017), URL <https://link.aps.org/doi/10.1103/RevModPhys.89.011004>.
- [98] P. Sierant, O. Dutta, and J. Zakrzewski (2018), *In preparation*.
- [99] A. K. Ekert, C. M. Alves, D. K. L. Oi, M. Horodecki, P. Horodecki, and L. C. Kwек, Phys. Rev. Lett. **88**, 217901 (2002), URL <http://link.aps.org/doi/10.1103/PhysRevLett.88.217901>.
- [100] P. Horodecki and A. Ekert, Phys. Rev. Lett. **89**, 127902 (2002), URL <http://link.aps.org/doi/10.1103/PhysRevLett.89.127902>.
- [101] J. Miszczyk, Z. Puchała, P. Horodecki, A. Uhlmann, and K. Życzkowski, Quant. Inf. Comp. **9**, 0103 (2009).
- [102] F. A. Bovino, G. Castagnoli, A. Ekert, P. Horodecki, C. M. Alves, and A. V. Sergienko, Phys. Rev. Lett. **95**, 240407 (2005), URL <http://link.aps.org/doi/10.1103/PhysRevLett.95.240407>.
- [103] A. J. Daley, H. Pichler, J. Schachenmayer, and P. Zoller, Phys. Rev. Lett. **109**, 020505 (2012), URL <http://link.aps.org/doi/10.1103/PhysRevLett.109.020505>.
- [104] H. Pichler, L. Bonnes, A. J. Daley, A. M. Läuchli, and P. Zoller, New Journal of Physics **15**, 063003 (2013), URL <http://stacks.iop.org/1367-2630/15/i=6/a=063003>.
- [105] A. Elben, B. Vermersch, M. Dalmonte, J. I. Cirac, and P. Zoller, Phys. Rev. Lett. **120**, 050406 (2018), URL <https://link.aps.org/doi/10.1103/PhysRevLett.120.050406>.
- [106] B. Vermersch, A. Elben, M. Dalmonte, J. I. Cirac, and P. Zoller, Phys. Rev. A **97**, 023604 (2018), URL <https://link.aps.org/doi/10.1103/PhysRevA.97.023604>.